

Joint Matrix Decomposition for Deep Convolutional Neural Networks Compression

Shaowu Chen, Jiahao Zhou, Weize Sun*, Lei Huang

arXiv:2107.04386v2 [cs.CV] 12 Jul 2021

Abstract—Deep convolutional neural networks (CNNs) with a large number of parameters requires huge computational resources, which has limited the application of CNNs on resources constrained appliances. Decomposition-based methods, therefore, have been utilized to compress CNNs in recent years. However, since the compression factor and performance are negatively correlated, the state-of-the-art works either suffer from severe performance degradation or have limited low compression factors. To overcome these problems, unlike previous works compressing layers separately, we propose to compress CNNs and alleviate performance degradation via joint matrix decomposition. The idea is inspired by the fact that there are lots of repeated modules in CNNs, and by projecting weights with the same structures into the same subspace, networks can be further compressed and even accelerated. In particular, three joint matrix decomposition schemes are developed, and the corresponding optimization approaches based on Singular Value Decomposition are proposed. Extensive experiments are conducted across three challenging compact CNNs and 3 benchmark data sets to demonstrate the superior performance of our proposed algorithms. As a result, our methods can compress the size of ResNet-34 by $22\times$ with slighter accuracy degradation compared with several state-of-the-art methods.

Index Terms—deep convolutional neural network, networks compression, model acceleration, joint matrix decomposition.

I. INTRODUCTION

In recent years, deep neural networks (DNNs), including deep convolutional neural networks (CNNs) and multilayer perceptron (MLPs), have achieved great successes in various areas, *e.g.*, noise reduction, object detection, matrix completion and signal processing [1]–[5]. To achieve good performance, very deep and complicated DNNs with a huge amount of parameters are developed [6]–[10], which is accompanied by billions of float point operations requirements and immense memory usage. Although high-performance servers with GPUs can meet the requirements of DNNs, it is problematic to deploy DNNs on resource-constrained platforms such as embedded or mobile devices [11]–[14], especially when a real-time forward inference is required. To tackle this problem, methods for networks compression are developed.

Shaowu Chen, Jiahao Zhou, Weize Sun and Lei Huang are with the Guangdong Key Laboratory of Intelligent Information Processing, College of Electronics and Information Engineering, Shenzhen University, Shenzhen 518060, China. (e-mail: shaowu-chen@foxmail.com; plus_chou@foxmail.com; proton198601@hotmail.com; lhuang8sasp@hotmail.com).

*Corresponding author: Weize Sun.

The work described in this paper was supported in part by the National Natural Science Foundation of China (NSFC) under Grant U1713217, U1913203 and 61807018, and in part by the Natural Science Foundation of Guangdong under Grant 2021A1515011706, and in part by the Foundation of Shenzhen under Grant JCYJ20190808122005605.

It has been found that weight matrices of fully connected (FC) layers and weight tensors of convolutional layers are of low rank [15], therefore the redundancy among these layers can be removed via decomposition methods. In [15]–[18], matrix decomposition alike methods are utilized to compress MLPs and CNNs in the one-shot manner or layer by layer progressively, in which a weight matrix \mathbf{W} is decomposed as $\mathbf{W} \approx \mathbf{U}\mathbf{V}$ where $\text{size}(\mathbf{U}) + \text{size}(\mathbf{V}) \ll \text{size}(\mathbf{W})$, and a relatively small compression factors (CF) are achieved at the cost of drop in accuracy. Recent works focus more on compressing CNNs, and to avoid unfolding 4-D weight tensors of convolutional layers into 2-D matrices to implement decomposition, tensor-decomposition-based methods [11][19]–[22] are introduced to compress CNNs. However, CNNs are much more compacted than MLPs because of the properties of parameters sharing, making the compression on CNNs challenging, thus previous works either compress CNNs with a small CF between $2\times$ and $5\times$ or suffer from severe performance degradation. Some methods proposed to alleviate degradation with a scheme associating properties of low rank and sparsity [23][24], in which $\mathbf{W} \approx \mathbf{U}\mathbf{V} + \mathbf{S}$, where \mathbf{S} is a highly sparse matrix. However, without support from particular libraries, the memory, storage and computation consumption of \mathbf{S} is as large as \mathbf{W} since $\text{size}(\mathbf{S}) = \text{size}(\mathbf{W})$, and the '0' elements as 2^n -bits numbers consume the same resources as those non-zero elements, not to mention the ones caused by \mathbf{U} and \mathbf{V} , making the method less practical.

To greatly compress CNNs without huge performance, we propose to compress CNNs via joint matrix decomposition. The main difference between our scheme and the state-of-the-art works is that we jointly decompose layers with relationship instead of compressing them separately. The idea is inspired by a basic observation that the widely used CNNs tend to adapt repeated modules to attain satisfying performance [6]–[10], making lots of convolutional layers sharing a same structure. Therefore, by projecting them into a same subspace, weight tensors can share identical factorized matrices and thus CNNs can be further compressed. Taking part of ResNet shown in the Figure 1 as an example, $\mathbf{W}_1^n, n = 1, \dots, N$ have the same structure and are placed in consistent position in the N BasicBlocks, thus might contain similar information and can be jointly decomposed, *i.e.*, $\mathbf{W}_1^n = \mathbf{G}^n \Sigma^n \mathbf{V} = \mathbf{U}^n \mathbf{V}$ where $\mathbf{U}^n = \mathbf{G}^n \Sigma^n$, and \mathbf{V} is identical for all $\mathbf{W}_1^n, n = 1, \dots, N$. In this manner, there are only almost half of matrices to be stored, *i.e.*, $\mathbf{U}^1, \mathbf{U}^2, \dots, \mathbf{U}^N$ and \mathbf{V} instead of $\mathbf{U}^1, \mathbf{U}^2, \dots, \mathbf{U}^N$ and $\mathbf{V}^1, \mathbf{V}^2, \dots, \mathbf{V}^N$, thus the requirement of storage and memory resources can be further reduced. After decomposing $\mathbf{W}_1^n, n = 1, \dots, N$, the similar procedure can implement

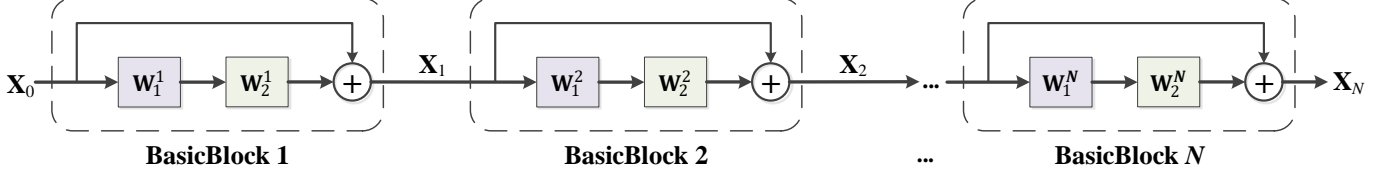


Fig. 1: A common network structure in ResNet. Here we assume that weights of convolutional layers are 2-D matrices instead of 4-D tensors for the convenience of explanation.

on $\mathbf{W}_2^n, n = 1, \dots, N$ as well. In our previous work [25], the relationship of layers was also taken into account but with clearly different idea, which considered a weight as the summation of a independent component and a shared one, and Tucker Decomposition or Tensor Train Decomposition [26] was utilized to factorized them, *i.e.*, $\mathbf{W}_m^n = \mathbf{W}_{m,i}^n + \mathbf{W}_{m,s} = \mathbf{G}_{m,i,1}^n * \mathbf{G}_{m,i,2}^n * \mathbf{G}_{m,i,3}^n + \mathbf{G}_{m,s,1}^n * \mathbf{G}_{m,s,2}^n * \mathbf{G}_{m,s,3}^n$, for $n = 1, \dots, N$, while in this paper we directly project weights into the same subspace via joint matrix decomposition.

In the above illustration, for convenience, it is supposed that the weight \mathbf{W} in convolutional layers are 2-D, but in fact they are 4-D tensors. To implement joint matrix decomposition, we firstly unfold the 4-D weight tensors into 2-D weight matrices following [18], and then introduce a novel Joint Singular Value Decomposition (JSVD) method to jointly decompose networks. Two JSVD algorithms for networks compression are proposed, referred as left shared JSVD (**LJSVD**) and right shared JSVD (**RJSVD**), respectively, according to the relative position of the identical factorized matrix. Besides, by combining LJSVD and RJSVD, another algorithm named as Binary JSVD (**Bi-JSVD**) is proposed as well, which can be considered as the generalized form of LJSVD and RJSVD. These algorithms can decompose a pre-trained CNN following a 'pre-train→decompose→fine-tune' criteria and train a compressed CNN from scratch by retaining the decomposed structure but randomly initializing weights. Furthermore, as a convolutional layers can be divided into two consecutive slimmer ones with less complexity by matrix decomposition, our methods can not only compress networks but also accelerate them without support from particular libraries.

The remainder of this paper is organised as follows. In Section II, we review some of the related works. In Section III, necessary notations and definitions are introduced firstly and then the joint matrix decomposition methods for networks compression are developed. Section IV presents extensive experiments evaluating the proposed methods, and the results are discussed in detail. Finally, a brief conclusion and future work are given in Section V.

II. RELATED WORKS

The decomposition methods for networks compression can be roughly divide into two categories, *i.e.*, matrix decomposition and tensor decomposition.

Matrix decomposition. In [15], weight tensors of convolutional layers are considered to be of low rank. Therefore, they were unfolded to 2-D matrices and then compressed via low-rank decomposition, in which the reconstruction ICA [27] and ridge regression with the squared exponential kernel were

used to predict parameters. Inspired by this, SVD and several clustering schemes were combined to achieve a $3.9\times$ weight reduction for a single convolutional layer in [16]. In [18], CNNs were compressed by removing the spatial or channel redundancy via low rank regularization, and a $5\times$ compression on AlexNet was achieved [18]. With the idea similar to knowledge distilling, some researches intentionally trained a larger or over-parameter network at first and then compressed it via matrix decomposition to meet the budget requirements, and thus made the compressed network performs better than the one trained from scratch directly under the same sizes [28]. To alleviate performance degradation and obtain higher compression factors, the property of sparsity was considered to be associated with low rank in [23][24], but these methods need supports from particular libraries to handle storage and the computation of the sparsity component. In [29], the sparsity was embedded with the low rank factorized matrices, which can be considered as the combination of unstructured pruning and matrix decomposition.

Tensor decomposition. The weight of a convolution layer is a 4-D tensor, therefore, tensor decomposition methods were applied to compress neural networks to achieve a higher compression factor. Some compact models were derived from tensor decomposition as well [30], such as the Inception model [31] and MobileNet [32] built with depthwise separable convolution. In [21], Tensor Train Decomposition (TTD) was extended from MLPs [19] to compress CNNs, and to achieve higher degree of reduction in sizes, weight tensors were folded to a higher dimensional tensors and then decomposed via TTD, in which a CNN were compressed by $4.02\times$ with a 2% loss of accuracy. However, since there are no associative law between convolution and contraction [33], when implementing forward inference, the original weight tensors have to be reconstructed using factorized tensors, which slows down the CNNs although the networks are compressed. In [11], spatial dimensions of a weight tensor were merged together to form a 3-D tensor, and then Tucker Decomposition was utilized to divide an original convolutional layer into 3 layers with less complexity. Note that in this case, the Tucker Decomposition is equal to TTD. To alleviate performance degradation caused by Tucker, [25] considered a weight tensor the summation of the independent and shared components, and applied Tucker Decomposition to each of them, respectively. In [33], Hybrid Tensor decomposition was utilized to achieve $4.29\times$ compression across a CNN on CIFAR-10 at a cost of 5.18% loss on accuracy, while TTD only brought $1.27\times$ loss, which means that TTD [21] is more suitable than HTD for compressing convolution layers.

III. METHODOLOGY

In this section, some necessary notations and definitions are introduced first, and then three different joint compression algorithms, namely, RJSVD, LJSVD and Bi-JSVD, are proposed.

A. Preliminaries

Notations. The notations and symbols used in this paper are introduced as follows. scalars, vectors, matrices (2-D) and tensors (with more than two dimensions) are denoted by italic, bold lower-case, bold upper-case and bold calligraphic symbols, respectively. Following the conventions of the Tensorflow, we represent an input tensor of one convolution layer as $\mathcal{X} \in \mathbb{R}^{H_1 \times W_1 \times I}$, the output as $\mathcal{Y} \in \mathbb{R}^{H_2 \times W_2 \times O}$, and the corresponding weight tensor as $\mathcal{W} \in \mathbb{R}^{F_1 \times F_2 \times I \times O}$, where H_1, W_1, H_2, W_2 are spatial dimensions, $F_1 \times F_2$ is the size of a filter, while I and O are the input and output depths, respectively [34]. Sometimes we would put the sizes of a tensor or matrix in its subscript to clarify the dimensions, for example, $\mathbf{W}_{I \times O}$ means $\mathbf{W} \in \mathbb{R}^{I \times O}$.

To jointly decompose a group of layers simultaneously, we further denote weights tensors or matrices with subscript and superscript such as \mathcal{W}_m^n , $n = 1, \dots, N$, $m = 1, \dots, M$, where m distinguishes different groups, and n distinguishes different elements inside a group. In other words, \mathcal{W}_m^n , $n = 1, \dots, N$ under the same m would be jointly decomposed. The Figure 1 is a concrete example with $M = 2$, and \mathbf{W}_1^n , $n = 1, 2, \dots, N$ is a group of weights that would be jointly decomposed, so as \mathbf{W}_2^n , $n = 1, 2, \dots, N$.

General unfolding. When applying matrix decomposition to compress convolutional layers, it is the first step to unfold weight tensors $\mathcal{W} \in \mathbb{R}^{F_1 \times F_2 \times I \times O}$ into 2-D matrices. Since the kernel sizes F_1 and F_2 are usually small values such as 3 or 5, following [18], we merge the first and third dimensions together and then the second and fourth ones. We refer to this operation as general unfolding, and denote it as **Unfold**(\cdot), which swaps the first and the third axes and then merge the first and second two dimension together respectively to produce $\text{Unfold}(\mathcal{W}) = \mathbf{W} \in \mathbb{R}^{F_1 I \times F_2 O}$.

General folding. We call the opposite operation of general unfolding as general folding, denoted as **Fold**(\cdot). By performing general folding on $\mathbf{W} \in \mathbb{R}^{F_1 I \times F_2 O}$, there would be $\text{Fold}(\mathbf{W}) = \mathcal{W} \in \mathbb{R}^{F_1 \times F_2 \times I \times O}$. For convenience, in the remainder of this article, **notations \mathcal{W} and \mathbf{W} would represent the general unfold weight tensor and the corresponding general folded matrix respectively**, unless there is particular statements.

Truncated rank- r SVD. The $\text{SVD}_r(\cdot)$ represents truncated rank- r SVD for networks compression, where r is the truncated rank. Note that it is a user-defined a given hyper-parameter to decide the number of singular values or vectors in the compressed model. Then we have $\mathbf{W}_{F_1 I \times F_2 O} \approx \mathbf{G}_{F_1 I \times r} \Sigma_{r \times r} \mathbf{V}_{r \times F_2 O} = \mathbf{U}_{F_1 I \times r} \mathbf{V}_{r \times F_2 O}$, where Σ is a diagonal matrix consists of singular values in descending order, \mathbf{G} , \mathbf{V} are orthogonal factorized matrices, $\mathbf{U} = \mathbf{G}\Sigma$, and $r \leq \min\{F_1 I, F_2 O\}$. After the decomposition, it is \mathbf{U} and \mathbf{V} that are stored instead of \mathbf{W} or \mathcal{W} , therefore the

network is compressed by a factor of $\frac{F_1 F_2 I O}{r(F_1 I + F_2 O)} \times$ where $r < \frac{F_1 F_2 I O}{(F_1 I + F_2 O)}$.

B. Proposed Algorithms

1) **Right Shared Joint SVD (RJSVD):** For $\mathcal{W}_m^n \in \mathbb{R}^{F_1 \times F_2 \times I \times O}$, $n = 1, \dots, N$ **under the same m** , we would like to jointly decompose these N weight tensors as follows:

$$\text{Unfold}(\mathcal{W}_m^n) = \mathbf{W}_m^n \approx \mathbf{G}_m^n \Sigma_m^n \mathbf{V}_m = \mathbf{U}_m^n \mathbf{V}_m \quad (1)$$

where $\mathbf{V}_m \in \mathbb{R}^{r_m^r \times F_2 O}$ are identical and shared for this group of \mathcal{W}_m^n , $n = 1, \dots, N$, while $\mathbf{U}_m^n \in \mathbb{R}^{F_1 I \times r_m^r} = \mathbf{G}_m^n \Sigma_m^n$ are different, and the r_m^r here is the truncated rank. In this manner, the sub-network is compressed by a factor of $\frac{F_1 F_2 I O N}{r_m^r (F_1 I + F_2 O)} \times$.

The optimization problem for (1) can be formulated as:

$$\begin{aligned} & \min_{\mathbf{U}_m^n, \mathbf{V}_m} \|\mathbf{W}_m^n - \mathbf{U}_m^n \mathbf{V}_m\|_2^2 \\ & \text{s.t. } \text{rank}(\mathbf{U}_m^n \mathbf{V}_m) \leq r_m^r \\ & \quad \text{for } n = 1, 2, \dots, N. \end{aligned} \quad (2)$$

Since it is difficult to optimize the rank, we take r_m^r as a given parameter, thus (2) can be rewritten as

$$\min_{\{\mathbf{U}_m^n\}_{n=1}^N, \mathbf{V}_m} \frac{1}{N} \sum_{n=1}^N \|\mathbf{W}_m^n - \mathbf{U}_m^n \mathbf{V}_m\|_2^2, \quad (3)$$

which can be solved by randomly initializing \mathbf{U}_m^n and \mathbf{V}_m at first and then update them alternatively as follow:

$$\begin{aligned} & (1) \text{ Given } \{\mathbf{U}_m^n\}_{n=1}^N, \\ & \quad \text{update } \mathbf{V}_m = \frac{1}{N} \sum_{n=1}^N (\mathbf{U}_m^n \mathbf{U}_m^n)^{-1} \mathbf{U}_m^n \mathbf{W}_m^n. \end{aligned}$$

$$\begin{aligned} & (2) \text{ Given } \mathbf{V}_m, \\ & \quad \text{update } \mathbf{U}_m^n = \mathbf{W}_m^n \mathbf{V}_m^T (\mathbf{V}_m \mathbf{V}_m^T)^{-1}, \text{ for } n = 1, 2, \dots, N. \end{aligned}$$

Alternatively, we could solve it in one single step by performing truncated rank- r_m^r SVD on the matrix produced by stacking \mathbf{W}_m^n , $n = 1, 2, \dots, N$ vertically:

$$\begin{bmatrix} \mathbf{U}_1^1 \\ \mathbf{U}_2^1 \\ \vdots \\ \mathbf{U}_N^1 \end{bmatrix}, \mathbf{V}_m = \text{SVD}_{r_m^r} \left(\begin{bmatrix} \mathbf{W}_1^1 \\ \mathbf{W}_2^1 \\ \vdots \\ \mathbf{W}_N^1 \end{bmatrix} \right). \quad (4)$$

The \mathbf{V}_m here is the right singular matrix which is shared and identical for \mathbf{W}_m^n , $n = 1, 2, \dots, N$, therefore we refer to the algorithm proposed for compressing CNNs based on (4) as **Right Shared Joint SVD (RJSVD)**. This algorithm can also accelerate forward inference of CNNs, because matrix decomposition shown above actually decompose a single convolution layer into two successive ones with less complexity, whose weight is a "vertical" one $\mathbf{U}_m^n = \text{fold}(\mathbf{U}_m^n) \in \mathbb{R}^{F_1 \times 1 \times I \times r_m^r}$ and a "horizontal" one $\mathbf{V}_m = \text{fold}(\mathbf{V}_m) \in \mathbb{R}^{1 \times F_2 \times r_m^r \times O}$, respectively, as shown in Figure 2 and proved as follows:

Proof. Let's temporarily get rid of superscripts and subscripts, and suppose there are a convolution layer with an input $\mathcal{X} \in \mathbb{R}^{F_1 \times F_2 \times I \times O}$, a weight tensor $\mathcal{W} \in \mathbb{R}^{F_1 \times F_2 \times I \times O}$ whose general unfolding matrix \mathbf{W} can be decompose into 2 matrices $\mathbf{U} \in \mathbb{R}^{F_1 I \times r}$ and $\mathbf{V} \in \mathbb{R}^{r \times F_2 O}$, therefore the convolutional output under settings of [1, 1] strides and 'SAME' padding is $\mathcal{Y} = \text{Conv}(\mathcal{W}, \mathcal{X}) \in \mathbb{R}^{1 \times 1 \times O}$. Defining $\text{vec}(\cdot)$ as vectorization operator, $\mathbf{X} = \text{unfold}(\mathcal{X}) \in \mathbb{R}^{F_1 I \times F_2 O}$ and

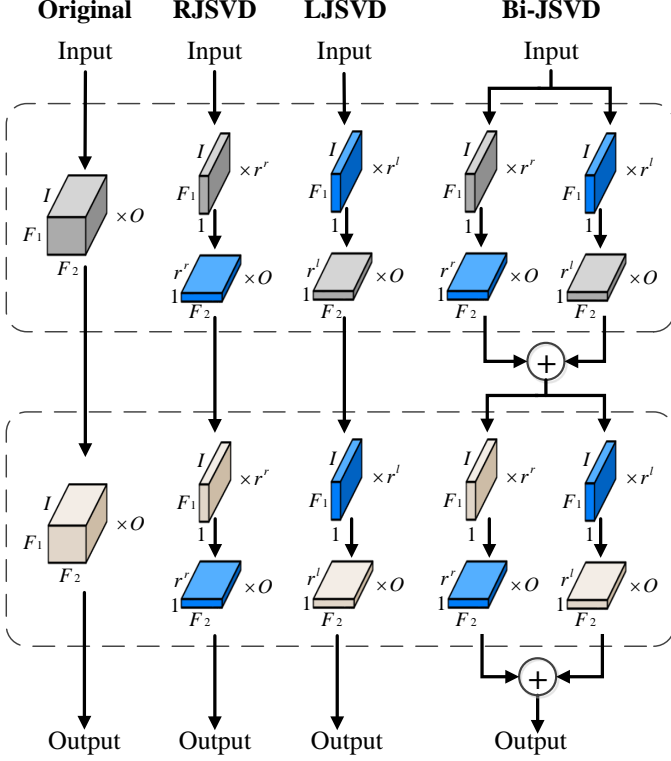


Fig. 2: Network structures of the original and the compressed networks with $N = 2$. RJSVD and LJSVD jointly divide each convolution layer into two consecutive slimmer ones with one half shared (the blue tensors), and Bi-JSVD can be seen as a combination of RJSVD and LJSVD.

$\mathbf{W}_{(:,i,F_2)} = \mathbf{W}[:, F_2 * (i-1) : F_2 * i]$, i.e., the i -th slice along the second axe with a length of F_2 , we have

$$\begin{aligned}
 \text{vec}(\mathbf{Y}) &= \text{vec}(\text{Conv}(\mathbf{W}, \mathbf{X})) \\
 &= \begin{bmatrix} \text{vec}(\mathbf{W}_{(:,1,F_2)})^T \\ \text{vec}(\mathbf{W}_{(:,2,F_2)})^T \\ \vdots \\ \text{vec}(\mathbf{W}_{(:,O,F_2)})^T \end{bmatrix} \text{vec}(\mathbf{X}) \\
 &= \begin{bmatrix} \text{vec}(\mathbf{U}\mathbf{V}_{(:,1,F_2)})^T \\ \text{vec}(\mathbf{U}\mathbf{V}_{(:,2,F_2)})^T \\ \vdots \\ \text{vec}(\mathbf{U}\mathbf{V}_{(:,O,F_2)})^T \end{bmatrix} \text{vec}(\mathbf{X}) \\
 &= \begin{bmatrix} \text{vec}(\mathbf{V}_{(:,1,F_2)})^T \\ \text{vec}(\mathbf{V}_{(:,2,F_2)})^T \\ \vdots \\ \text{vec}(\mathbf{V}_{(:,O,F_2)})^T \end{bmatrix} \text{vec}(\mathbf{U}^T \mathbf{X}) \\
 &= \begin{bmatrix} \text{vec}(\mathbf{V}_{(:,1,F_2)})^T \\ \text{vec}(\mathbf{V}_{(:,2,F_2)})^T \\ \vdots \\ \text{vec}(\mathbf{V}_{(:,O,F_2)})^T \end{bmatrix} \text{vec}(\text{Conv}(\mathbf{U}, \mathbf{X})) \\
 &= \text{vec}(\text{Conv}(\mathbf{V}, \text{Conv}(\mathbf{U}, \mathbf{X}))), \tag{5}
 \end{aligned}$$

therefore, $\text{Conv}(\mathbf{W}, \mathbf{X}) = \text{Conv}(\mathbf{V}, \text{Conv}(\mathbf{U}, \mathbf{X}))$ \square

A more complicated case with a different sizes of $\mathbf{X} \in \mathbb{R}^{H \times W \times I}$ and strides $[s, s]$ can be proven in a similar way, thus in the compressed CNN, it is not necessary to reconstruct \mathbf{W}

as in [21][33] in the forward inference, instead we only need to replace the original convolution layer with two consecutive factorized ones, where the first one has the weight tensor $\mathbf{U} \in \mathbb{R}^{F_1 \times 1 \times I \times r}$ with strides $[s, 1]$ and the second one $\mathbf{V} \in \mathbb{R}^{1 \times F_2 \times r \times O}$ with strides $[1, s]$. In this manner, CNNs are not only be compressed but also accelerated in the inference period, since the complexity of a convolutional layer is dropped from $\mathcal{O}(H'W'F_1F_2IO)$ to $\mathcal{O}(H'WF_1Ir_m^r + H'W'F_2r_m^rO)$ where $H' \times W'$ is the spatial sizes of the convolutional output. After decomposition, fine-tuning can be conducted to recover performance, and the whole process of RJSVD is shown in the Algorithm 1.

The compression factor (**CF**) in this algorithm can be defined now. Denoting the number of uncompressed parameters such as those in the soft-max layer, BN layers, and uncompressed layers as $\#\text{Other}$ where $\#$ means sizes of parameters, the compression factor is

$$\text{CF} = \frac{\sum_{m=1}^M \sum_{n=1}^N \#\mathbf{W}_m^n + \#\text{Other}}{\sum_{m=1}^M (\#\mathbf{V}_m + \sum_{n=1}^N \#\mathbf{U}_m^n) + \#\text{Other}}. \tag{6}$$

Algorithm 1: RJSVD

Input: A pre-trained CNN with weight tensors $\{\{\mathbf{W}_m^n\}_{n=1}^N\}_{m=1}^M$, and target ranks $\{r_m^r\}_{m=1}^M$.

for $m = 1, 2, \dots, M$ **do**

Obtain $\{\mathbf{U}_m^n\}_{n=1}^N, \mathbf{V}_m$ according to the equation (4).

$\mathbf{V}_m = \text{fold}(\mathbf{V}_m)$.

for $n = 1, 2, \dots, N$ **do**

$\mathbf{U}_m^n = \text{fold}(\mathbf{U}_m^n)$.

Replace the original convolutional layer \mathbf{W}_m^n with two compressed ones \mathbf{U}_m^n and \mathbf{V}_m .

end

end

Fine-tune the compressed CNN.

Output: The compressed CNN and its weights $\mathbf{U}_m^n, \mathbf{V}_m$.

2) *Left Shared Joint SVD (LJSVD):* In the RJSVD, the right singular matrix is shared to further compress CNNs, which enables weight typing across layers. Following the same idea, it is natural to derived **Left Shared Joint SVD (LJSVD)** by sharing the left factorized matrix, which is:

$$\text{Unfold}(\mathbf{W}_m^n) = \mathbf{W}_m^n \approx \mathbf{U}_m \mathbf{V}_m^n, \tag{7}$$

where $\mathbf{U}_m \in \mathbb{R}^{F_1 I \times r_m^l}$ are identical and shared for a group of $\mathbf{W}_m^n, n = 1, \dots, N$, while $\mathbf{V}_m^n \in \mathbb{R}^{r_m^l \times F_2 O}$ is different. The decomposed structure derived by LJSVD is shown in the Figure 2.

Similar to (3), the optimization problem of LJSVD can be formulated as:

$$\min_{\{\mathbf{U}_m^n\}_{n=1}^N, \mathbf{V}_m} \frac{1}{N} \sum_{n=1}^N \|\mathbf{W}_{n,m} - \mathbf{U}_m \mathbf{V}_m^n\|_2^2, \tag{8}$$

which can be solved by performing truncated rank- r_m^l SVD on the matrix produced by stacking $\mathbf{W}_m^n, n = 1, 2, \dots, N$ horizontally:

$$\mathbf{U}_m, [\mathbf{V}_m^1, \mathbf{V}_m^2, \dots, \mathbf{V}_m^N] = \text{SVD}_{r_m^l}([\mathbf{W}_m^1, \mathbf{W}_m^2, \dots, \mathbf{W}_m^N]). \quad (9)$$

The concrete steps are shown in the Algorithm 2. With this algorithm, the complexity of a convolutional layer will drop from $\mathcal{O}(H'W'F_1F_2IO)$ to $\mathcal{O}(H'WF_1Ir_m^l + H'W'F_2r_m^lO)$. And similar to the (6), the CF for LJSVD is

$$\text{CF} = \frac{\sum_{m=1}^M \sum_{n=1}^N \#\mathcal{W}_m^n + \#\text{Other}}{\sum_{m=1}^M (\#\mathcal{U}_m + \sum_{n=1}^N \#\mathcal{V}_m^n) + \#\text{Other}}. \quad (10)$$

Algorithm 2: LJSVD

Input: A pre-trained CNN with weight tensors $\{\{\mathcal{W}_m^n\}_{n=1}^N\}_{m=1}^M$, and target ranks $\{r_m^l\}_{m=1}^M$.

for $m = 1, 2, \dots, M$ **do**

- Obtain $\mathbf{U}_m, \{\mathbf{V}_m^n\}_{n=1}^N$ according to the equation (9).
- $\mathcal{U}_m = \text{fold}(\mathbf{V}_m)$.
- for** $n = 1, 2, \dots, N$ **do**

 - $\mathcal{V}_m^n = \text{fold}(\mathbf{V}_m^n)$.
 - Replace the original convolutional layer \mathcal{W}_m^n with two compressed ones \mathcal{U}_m and \mathcal{V}_m^n .

- end**

end

Fine-tune the compressed CNN.

Output: The compressed CNN and its weights $\mathcal{U}_m, \mathcal{V}_m^n$.

3) *Binary Joint SVD (Bi-JSVD)*: The RJSVD and LJSVD jointly project weight tensors of repeated layers into a same subspace by sharing the right factorized matrices or the left ones, and in this section, we would like to combine RJSVD and LJSVD together to generate **Binary Joint SVD (Bi-JSVD)**, which is

$$\text{Unfold}(\mathcal{W}_m^n) = \mathbf{W}_m^n \approx \mathbf{U}_m^n \mathbf{V}_m + \mathbf{U}_m \mathbf{V}_m^n, \quad (11)$$

where $\mathbf{U}_m^n \in \mathbb{R}^{F_1I \times r_m^r}, \mathbf{V}_m \in \mathbb{R}^{r_m^r \times F_2O}, \mathbf{U}_m \in \mathbb{R}^{F_1I \times r_m^l}, \mathbf{V}_m^n \in \mathbb{R}^{r_m^l \times F_2O}$. It is worth noting that Bi-JSVD is the generalization of RJSVD and LJSVD. In other words, RJSVD is a particular case of Bi-JSVD when $r_m^l = 0$, and so as LJSVD when $r_m^r = 0$.

The optimization problem for (11) can be formulated as:

$$\min_{\{\mathbf{U}_m^n, \mathbf{V}_m^n\}_{n=1}^N, \mathbf{U}_m, \mathbf{V}_m} \frac{1}{N} \sum_{n=1}^N \|\mathbf{W}_{n,m} - \mathbf{U}_m^n \mathbf{V}_m - \mathbf{U}_m \mathbf{V}_m^n\|_2^2. \quad (12)$$

It would be inefficient to solve this with the simultaneous optimization on $\{\mathbf{U}_m^n\}_{n=1}^N, \mathbf{V}_m$, and $\mathbf{U}_m, \{\mathbf{V}_m^n\}_{n=1}^N$, therefore we proposed to solve it alternatively and iteratively as follows:

(1) Given $\mathbf{U}_m, \{\mathbf{V}_m^n\}_{n=1}^N$, let

$$\widehat{\mathbf{W}}_m^n = \mathbf{W}_m^n - \mathbf{U}_m \mathbf{V}_m^n, \text{ for } n = 1, \dots, N, \quad (13)$$

then we have

$$\begin{bmatrix} \mathbf{U}_m^1 \\ \mathbf{U}_m^2 \\ \vdots \\ \mathbf{U}_m^N \end{bmatrix}, \mathbf{V}_m = \text{SVD}_{r_m^l} \left(\begin{bmatrix} \widehat{\mathbf{W}}_m^1 \\ \widehat{\mathbf{W}}_m^2 \\ \vdots \\ \widehat{\mathbf{W}}_m^N \end{bmatrix} \right). \quad (14)$$

(2) Given $\{\mathbf{U}_m^n\}_{n=1}^N, \mathbf{V}_m$, let

$$\widehat{\mathbf{W}}_m^n = \mathbf{W}_m^n - \mathbf{U}_m^n \mathbf{V}_m, \text{ for } n = 1, \dots, N, \quad (15)$$

then we have

$$\mathbf{U}_m, [\mathbf{V}_m^1, \mathbf{V}_m^2, \dots, \mathbf{V}_m^N] = \text{SVD}_{r_m^l}([\widehat{\mathbf{W}}_m^1, \widehat{\mathbf{W}}_m^2, \dots, \widehat{\mathbf{W}}_m^N]). \quad (16)$$

The decomposition will be converged by repeating the above steps for K times, and then the fine-tuning on the compressed network can be employed to recover its performance, which is summarized in the Algorithm 3. The CF for Bi-JSVD is

$$\text{CF} = \frac{\sum_{m=1}^M \sum_{n=1}^N \#\mathcal{W}_m^n + \#\text{Other}}{\sum_{m=1}^M (\#\mathcal{V}_m + \#\mathcal{U}_m + \sum_{n=1}^N (\#\mathcal{U}_m^n + \#\mathcal{V}_m^n)) + \#\text{Other}}, \quad (17)$$

and the complexity of a compressed convolutional layer is $\mathcal{O}((H'WF_1I + H'W'F_2O)(r_m^l + r_m^r))$.

Algorithm 3: Bi-JSVD

Input: A pre-trained CNN with weight tensors $\{\{\mathcal{W}_m^n\}_{n=1}^N\}_{m=1}^M$, target ranks $\{r_m^r, r_m^l\}_{m=1}^M$, and iteration times K .

for $m = 1, 2, \dots, M$ **do**

- Initialization: $\mathbf{U}_m = 0, \{\mathbf{V}_m^n\}_{n=1}^N = 0$.
- for** $(k = 0; k < K; k++)$ **do**

 - Update $\{\mathbf{U}_m^n\}_{n=1}^N, \mathbf{V}_m$ according to (13) (14).
 - Update $\mathbf{U}_m, \{\mathbf{V}_m^n\}_{n=1}^N$ according to (15) (16).

- end**
- $\mathcal{U}_m = \text{fold}(\mathbf{U}_m)$.
- $\mathcal{V}_m = \text{fold}(\mathbf{V}_m)$.
- for** $n = 1, 2, \dots, N$ **do**

 - $\mathcal{U}_m^n = \text{fold}(\mathbf{U}_m^n)$.
 - $\mathcal{V}_m^n = \text{fold}(\mathbf{V}_m^n)$.
 - Replace the original convolutional layer \mathcal{W}_m^n with two parallel compressed sub-networks $\mathcal{U}_m^n, \mathcal{V}_m$ and $\mathcal{U}_m, \mathcal{V}_m^n$ as shown in the Figure 2.

- end**

Fine-tune the compressed CNN.

Output: The compressed CNN and its weights $\mathcal{U}_m, \mathcal{V}_m^n, \mathcal{U}_m^n, \mathcal{V}_m$.

IV. EXPERIMENTS

To validate the effectiveness of the proposed algorithms, we conducted extensive experiments on various benchmark data sets and several widely used networks with different depths. The proposed algorithms are adopted to compressed

layer name	output size	ResNet-18	ResNet-34	ResNet-50
conv1 (original)	32×32		$3 \times 3, 64$, stride 1	
conv2_x (original)	32×32	$\begin{bmatrix} 3 \times 3, 64 \\ 3 \times 3, 64 \end{bmatrix} \times 2$	$\begin{bmatrix} 3 \times 3, 64 \\ 3 \times 3, 64 \end{bmatrix} \times 3$	$\begin{bmatrix} 1 \times 1, 64 \\ 3 \times 3, 64 \\ 1 \times 1, 256 \end{bmatrix} \times 3$
conv3_x (decom)	16×16	$\begin{bmatrix} 3 \times 3, 128 \\ 3 \times 3, 128 \end{bmatrix} \times 2$	$\begin{bmatrix} 3 \times 3, 128 \\ 3 \times 3, 128 \end{bmatrix} \times 4$	$\begin{bmatrix} 1 \times 1, 128 \\ 3 \times 3, 128 \\ 1 \times 1, 512 \end{bmatrix} \times 4$
conv4_x (decom)	8×8	$\begin{bmatrix} 3 \times 3, 256 \\ 3 \times 3, 256 \end{bmatrix} \times 2$	$\begin{bmatrix} 3 \times 3, 256 \\ 3 \times 3, 256 \end{bmatrix} \times 6$	$\begin{bmatrix} 1 \times 1, 256 \\ 3 \times 3, 256 \\ 1 \times 1, 1024 \end{bmatrix} \times 6$
conv5_x (decom)	4×4	$\begin{bmatrix} 3 \times 3, 512 \\ 3 \times 3, 512 \end{bmatrix} \times 2$	$\begin{bmatrix} 3 \times 3, 512 \\ 3 \times 3, 512 \end{bmatrix} \times 3$	$\begin{bmatrix} 1 \times 1, 512 \\ 3 \times 3, 512 \\ 1 \times 1, 2048 \end{bmatrix} \times 3$
average pool, 10-d fc for CIFAR-10/100-d fc for CIFAR-100, softmax				

Table I: Architecture of CNNs for CIFAR-10 and CIFAR-100. Layers remarked with "original" will not be decomposed in the following experiments, while those remarked with "decom" will be decomposed.

networks and we compare the results with some state-of-the-art decomposition-based compression methods. All the experiments are performed on one TITAN Xp GPU under Tensorflow1.15 and Ubuntu18.04.¹

A. Evaluation on CIFAR-10 and CIFAR-100

1) *Overall settings:* In this section, we evaluate the proposed methods on CIFAR-10 and CIFAR-100 [35]. Both data sets have 60,000 $32 \times 32 \times 3$ images, including 50,000 training images and 10,000 testing images. The former contains 10 classes, while the latter includes 100 categories, and thus is more challenging for classification. For data preprocessing, all the images are normalized with $mean = [0.4914, 0.4822, 0.4465]$ and standard deviation $std = [0.2023, 0.1994, 0.2010]$. For data augmentation, a 32×32 random crop is adopted on the zero-padded 40×40 training images followed by a random horizontal flip.

Networks. We evaluate the proposed method on the widely used ResNet with various depth, *i.e.*, ResNet-18, ResNet-34, ResNet-50. The reasons for choosing them are that the widely used ResNet is a typical representative of architectures that adopts the idea of repeated module designing, and it's hard to compress these compact networks [36] thus the ability of the proposed methods can be clearly presented. The architectures and Top-1 accuracies of the baseline CNNs are shown in the Table I and II, respectively. We randomly initialize the weights with truncated normal initializer by setting the standard deviation to 0.01, and the L2 regularization is used with a weight decay of 5e-4. The SGD is used as optimizer with a momentum of 0.9 to train the CNNs for 300 epochs. The batch size for ResNet-18 and ResNet-34 is 256, and 128 for ResNet-50 because of the limitation of graphics memory. The learning rate starts from 0.1 and is divided by 10 in the 140th, 200th and 250th epochs.

Methods for comparison. To evaluate the effectiveness of the proposed algorithms, three state-of-the-art methods, including one matrix-decomposition-based method, Tai *et.al* [18], and two tensor-decomposition-based ones, Tucker [11], and NC_CTD [25], are employed for comparison.

¹The codes are available at <https://github.com/ShaowuChen/JointSVD>.

CNN	CIFAR-10		CIFAR-100	
	Acc. (%)	Size (m)	Acc. (%)	Size (m)
ResNet-18	94.80	11.16	70.73	11.21
ResNet-34	95.11	21.27	75.81	21.31
ResNet-50	95.02	23.50	75.67	23.69

Table II: Top-1 accuracies and parameter sizes of the baseline CNNs on CIFAR-10 and CIFAR-100. "Acc." means "Accuracy".

2) *Tuning the Parameter K:* In the beginning, we first determine the iteration number K for Bi-JSVD as it might affect the quality of the initialization after decomposition and before fine-tuning. Empirically, a more accurate approximation in decomposition would bring better performance after fine-tuning, making K a inconspicuous but vital hyper-parameter. A extremely large K can make sure of the convergence for decomposition, but it would lead to a high computational time in training. To find out a suitable K , we conduct experiments on ResNet-34 for CIFAR-10, and the raw accuracy of the decomposed network before fine-tuning is used for evaluation..

Settings. We decompose the sub-networks $conv_i_x$ for $i = 3, 4, 5$ in the Table I except the $conv1$ and $conv2_x$, for the reason that the number of parameters in them are relatively small and decomposing them would bring relatively server accumulated error. In each sub-networks ' $conv_i_x$ ' for $i = 3, 4, 5$, the first convolutional layer of the first block has only half of the input depth (**HID layer**) comparing with the one in other blocks, thus they are not included for Bi-JSVD but decomposed by matrix method separately as in [18]. The CF and iteration times is set to 13.9 and $K \in \{10, 30, 50, 70\}$, respectively, and we set the proportion of LJSVD, p ($p = \frac{r_m^l}{r_m^l + r_m^r}$), in Bi-JSVD to $p = 0.3, 0.5, 0.7, 0.9$.

Results and analysis. The results are shown in the Table III. It is shown that $K = 30$ and $K = 70$ would bring relatively high raw accuracy, and the gaps between them are insignificant. Therefore, K will set to 30 in the following experiments to obtain high raw accuracy with less complexity. Furthermore, it seems the p or the proportion of LJSVD or RJSVD in Bi-JSVD would affect the raw accuracy of the

compressed network, but to give a conclusion on how it affects the final performance, more experiments are needed, and we will discover it in the following sections.

K	<i>p</i>			
	0.3	0.5	0.7	0.9
10	57.64%	53.44%	51.04%	42.69%
30	58.12%	56.43%	51.75%	44.01%
50	57.33%	56.77%	50.23%	43.45%
70	57.65%	56.85%	49.47%	44.13%

Table III: Raw accuracies of compressed ResNet-34 with Bi-JSVD on CIFAR-10 before fine-tuning.

3) *Performance Comparison*: To conduct performance comparison, conv1 and conv2_x in all CNNs will not be decomposed as discussed in IV-A2. In ResNet-18 and ResNet-34, we compare the proposed methods with Tai *et.al* [18], Tucker [11], and NC_CTD [25] following the 'pre-train→decompose→fine-tune' criteria. To see the gap of performance clearly, the CF is set to be relatively large, which is roughly from 14 to 20. In ResNet-50, since there are lots of 1×1 convolutional layers, and the weight tensors of them with sizes $1 \times 1 \times I \times O$ are actually 2-D matrices, making the Tucker or tensor decomposition equal to matrix decomposition, thus only the Tai *et.al* [18] is used as baseline. However, since BottleNeck makes ResNet-50 very compact, we set the CF to be 6, which is almost the possible largest one. For rank setting, we take Tai *et.al* as the anchor, *i.e.*, a proportion equal for each layer are set to determine ranks for Tai *et.al* and to get the CF, with which the proportion for ranks in Tucker, NC_CTD and our methods can be calculated to maintain the same CF. In NC_CTD, since the proportion of the shared component and independent component affects the final performance, without loss of generality, we set it to be 1 : 1 as well as 2 : 1 and use the results with better performance..

For LJSVD and Bi-JSVD, as in the Section IV-A2, the HID layers with half of input depth will be decomposed via Tai *et.al* separately instead of LJSVD and Bi-JSVD. However, since RJSVD stacks folded weights vertically, it is compatible with HID layers, therefore, to comprehensively evaluate RJSVD, HID layers is included for jointly decomposition in the **RJSVD-1** experiments, while in the **RJSVD-2**, the HID layers are decomposed via Tai *et.al* [18] separately. To answer the query posted in the last experiment, *i.e.*, how $p = \frac{r_m^l}{r_m^l + r_m^r}$ in Bi-JSVD affects the performance of the compress networks, we set different p and name the methods as **Bi-JSVDp**, for $p = 0.3, 0.5, 0.7$.

There are 12 groups of experiment implemented in total, and to conduct a fair comparison and avoid early convergence, in the fine-tuning period, we use the same training setting as training the baseline CNNs in the section IV-A1 for all the methods, except that all the batch sizes are set to 128, and no other tricks are used. All the experiments are conducted repeatedly for 3 times to obtain average performance, and the highest accuracy recorded during fine-tuning, which indicates the potential of the corresponding models, is presented as well.

CNN & acc. (%)	CF (×)	Method	Raw acc. (%)	Acc. (%) (mean±std)	Best acc. (%)
ResNet-18	17.76	Tai <i>et.al</i> [18]	10.31	92.49±0.23	92.93
		Tucker [11]	23.77	91.93±0.13	92.41
		NC_CTD [25]	23.51	92.20±0.29	92.80
		LJSVD	11.44	92.88±0.08	93.00
		RJSVD-1	10.00	93.19±0.04	93.36
	94.80	RJSVD-2	10.27	92.75±0.09	93.09
		Bi-JSVD0.3	13.76	92.81±0.06	92.91
		Bi-JSVD0.5	13.09	92.70±0.11	92.80
		Bi-JSVD0.7	13.64	93.11±0.06	93.32
		Tai <i>et.al</i> [18]	54.42	93.55±0.08	93.83
ResNet-34	11.99	Tucker [11]	57.51	92.42±0.29	92.84
		NC_CTD [25]	54.15	92.85±0.25	93.34
		LJSVD	50.15	93.62±0.10	93.98
		RJSVD-1	30.53	93.75±0.07	94.22
		RJSVD-2	42.43	93.47±0.12	93.80
	22.07	Bi-JSVD0.3	52.84	93.77±0.17	94.15
		Bi-JSVD0.5	48.45	93.49±0.07	93.73
		Bi-JSVD0.7	52.31	93.84±0.09	94.16
		Tai <i>et.al</i> [18]	12.93	93.66±0.13	93.98
		Tucker [11]	19.73	92.83±0.07	93.06
ResNet-50	95.11	NC_CTD [25]	19.12	92.98±0.15	93.35
		LJSVD	15.96	93.97±0.10	94.07
		RJSVD-1	10.21	93.82±0.07	94.00
		RJSVD-2	12.97	93.77±0.03	93.95
		Bi-JSVD0.3	17.38	93.66±0.05	93.88
	13.92	Bi-JSVD0.5	16.87	93.69±0.09	93.98
		Bi-JSVD0.7	15.83	93.77±0.13	94.09
		Tai <i>et.al</i> [18]	49.34	93.95±0.05	94.12
		Tucker [11]	64.13	93.04±0.21	93.39
		NC_CTD [25]	60.12	93.30±0.13	93.69
ResNet-50	6.48	LJSVD	39.53	94.39±0.15	94.61
		RJSVD-1	46.38	94.23±0.23	94.73
		RJSVD-2	45.60	93.94±0.06	94.12
		Bi-JSVD0.3	58.12	94.17±0.09	94.41
		Bi-JSVD0.5	56.43	94.08±0.06	94.32
	95.02	Bi-JSVD0.7	51.75	94.02±0.19	94.34
		Tai <i>et.al</i> [18]	20.24	92.38±0.31	92.96
		LJSVD	12.07	93.08±0.17	93.37
		RJSVD-1	13.85	93.28±0.09	93.58
		RJSVD-2	20.48	92.75±0.28	93.26
ResNet-50	5.37	Bi-JSVD0.3	16.11	92.97±0.12	93.30
		Bi-JSVD0.5	13.46	92.90±0.15	93.19
		Bi-JSVD0.7	10.73	92.84±0.26	93.49
		Tai <i>et.al</i> [18]	28.40	92.99±0.42	93.44
		LJSVD	22.67	93.39±0.18	93.81
	22.07	RJSVD-1	24.94	92.97±0.10	93.33
		RJSVD-2	34.46	93.24±0.11	93.41
		Bi-JSVD0.3	32.18	92.86±0.19	93.17
		Bi-JSVD0.5	32.39	93.08±0.21	93.50
		Bi-JSVD0.7	35.34	93.06±0.09	93.28

Table IV: Comparison of compressed ResNet following the 'pre-train→decompose→fine-tune' criteria on CIFAR-10. "Raw acc." means accuracy before fine-tuning. "Acc." and "Best acc." represents the average accuracy and best accuracy after fine-tuning among repeated experiments, respectively.

Results. The results are shown in Table IV and V. To observe how p affect the Bi-JSVD, we plot the curves of the average and best performance with $p = [0, 0.3, 0.5, 0.7, 1]$ under different CFs in the Figures 3 and 4. Note that RJSVD-2, LJSVD are equivalent to Bi-JSVD0 and Bi-JSVD1, respectively.

Analysis. From the results, we summarize several important observations:

- (i) All the proposed methods outperform the baselines after fine-tuning in most cases, and CFs such as 22× much

CNN & acc. (%)	CF (x)	Method	Raw acc. (%)	Acc. (%) (mean \pm std)	Best acc. (%)
16.61	Tai <i>et.al</i> [18]	2.07	71.15 \pm 0.16	71.86	
	Tucker [11]	7.69	71.54 \pm 0.26	72.62	
	NC_CTD [25]	3.94	72.02\pm0.13	72.74	
	LJSVD	2.43	71.63 \pm 0.29	72.36	
	RJSVD-1	1.67	72.02\pm0.30	72.87	
	RJSVD-2	2.97	71.35 \pm 0.19	71.78	
	Bi-JSVD0.3	3.78	71.56 \pm 0.13	72.04	
ResNet-18	Bi-JSVD0.5	4.14	71.93 \pm 0.21	72.55	
	Bi-JSVD0.7	3.95	71.61 \pm 0.11	72.28	
	Tai <i>et.al</i> [18]	9.22	73.63 \pm 0.17	74.42	
	Tucker [11]	26.33	72.24 \pm 0.17	72.78	
	NC_CTD [25]	22.02	72.88 \pm 0.11	73.46	
	LJSVD	6.42	74.16\pm0.33	75.02	
	RJSVD-1	5.95	74.00 \pm 0.10	74.27	
70.73	RJSVD-2	8.88	73.71 \pm 0.14	74.17	
	Bi-JSVD0.3	7.79	74.00 \pm 0.13	74.43	
	Bi-JSVD0.5	8.31	73.71 \pm 0.17	73.93	
	Bi-JSVD0.7	7.77	73.76 \pm 0.15	74.21	
	Tai <i>et.al</i> [18]	2.30	73.30 \pm 0.15	73.56	
	Tucker [11]	5.66	73.53 \pm 0.14	73.81	
	NC_CTD [25]	3.77	73.91 \pm 0.27	74.59	
11.47	LJSVD	4.75	74.39\pm0.02	74.92	
	RJSVD-1	3.45	73.96 \pm 0.16	74.31	
	RJSVD-2	4.33	73.81 \pm 0.13	74.33	
	Bi-JSVD0.3	3.29	73.88 \pm 0.15	74.38	
	Bi-JSVD0.5	5.12	74.03 \pm 0.12	74.55	
	Bi-JSVD0.7	5.19	74.05 \pm 0.31	74.62	
	Tai <i>et.al</i> [18]	6.35	75.29 \pm 0.23	75.50	
21.11	Tucker [11]	19.69	74.07 \pm 0.44	75.18	
	NC_CTD [25]	17.51	74.53 \pm 0.12	75.18	
	LJSVD	10.66	75.84\pm0.16	76.26	
	RJSVD-1	6.09	75.43 \pm 0.07	75.76	
	RJSVD-2	10.83	75.34 \pm 0.37	75.90	
	Bi-JSVD0.3	13.52	75.84\pm0.21	76.48	
	Bi-JSVD0.5	13.47	75.61 \pm 0.11	75.85	
ResNet-34	Bi-JSVD0.7	10.73	75.84\pm0.37	76.47	
	Tai <i>et.al</i> [18]	6.35	75.29 \pm 0.23	75.50	
	Tucker [11]	19.69	74.07 \pm 0.44	75.18	
	NC_CTD [25]	17.51	74.53 \pm 0.12	75.18	
	LJSVD	10.66	75.84\pm0.16	76.26	
	RJSVD-1	6.09	75.43 \pm 0.07	75.76	
	RJSVD-2	10.83	75.34 \pm 0.37	75.90	
75.81	Bi-JSVD0.3	13.52	75.84\pm0.21	76.48	
	Bi-JSVD0.5	13.47	75.61 \pm 0.11	75.85	
	Bi-JSVD0.7	10.73	75.84\pm0.37	76.47	
	Tai <i>et.al</i> [18]	7.65	74.36 \pm 0.23	74.90	
	LJSVD	3.71	75.04 \pm 0.32	75.63	
	RJSVD-1	2.18	73.56 \pm 0.41	74.52	
	RJSVD-2	2.66	73.51 \pm 0.55	74.59	
6.21	Bi-JSVD0.3	3.00	74.79 \pm 0.14	75.14	
	Bi-JSVD0.5	2.65	74.25 \pm 0.27	74.65	
	Bi-JSVD0.7	3.34	74.47 \pm 0.09	74.92	
	Tai <i>et.al</i> [18]	24.67	75.09 \pm 0.31	75.71	
	LJSVD	5.57	75.67\pm0.45	76.64	
	RJSVD-1	4.72	74.43 \pm 0.46	75.49	
	RJSVD-2	8.02	74.36 \pm 0.33	74.81	
75.67	Bi-JSVD0.3	6.71	75.30 \pm 0.41	76.06	
	Bi-JSVD0.5	5.76	74.81 \pm 0.62	75.81	
	Bi-JSVD0.7	5.06	75.01 \pm 0.30	75.93	
	Tai <i>et.al</i> [18]	24.67	75.09 \pm 0.31	75.71	
	LJSVD	5.57	75.67\pm0.45	76.64	
5.19	RJSVD-1	4.72	74.43 \pm 0.46	75.49	
	RJSVD-2	8.02	74.36 \pm 0.33	74.81	
	Bi-JSVD0.3	6.71	75.30 \pm 0.41	76.06	
	Bi-JSVD0.5	5.76	74.81 \pm 0.62	75.81	
	Bi-JSVD0.7	5.06	75.01 \pm 0.30	75.93	

Table V: Comparison of compressed ResNet following the 'pre-train \rightarrow decompose \rightarrow fine-tune' criteria on CIFAR-100.

higher than previous works are achieved with relatively slight performance degradation, which demonstrates the effectiveness of joint decomposition scheme. Moreover, it is shown that a deeper network with more layers for joint decomposition would expand the advantages of the proposed methods in alleviating performance degradation, and in the experiments on CIFAR-100, the advantages of our methods are further enlarged by the challenging task as well. For example, the accuracy of the ResNet-18 jointly decomposed by LJSVD on CIFAR-100 under CF = 11.47 is 1.92% higher than Tucker and 0.53% higher than Tai *et.al.*. Furthermore, in the experiments for ResNet-34 on CIFAR-100 with

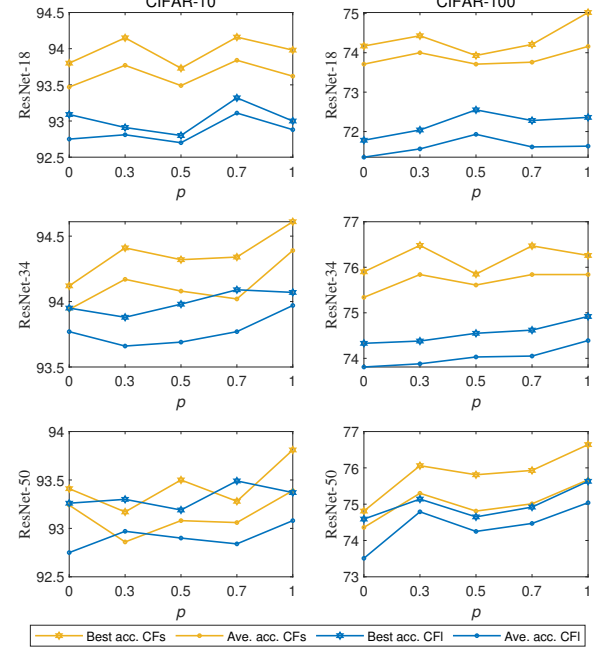


Fig. 3: The performance of Bi-JSVD for pre-trained CNNs under different p . "Ave. acc.", "Best acc.", "CFs" and "CFI" means Average accuracy, Best accuracy, the smaller CF and the larger one for each CNN shown in the TABLE IV and V, respectively.

CR=13.55, there are not significant loss in accuracy for our methods.

- (ii) Among the proposed methods, LJSVD is most outstanding one, as it achieves the highest average accuracy in 8 out of 12 groups. The RJSVD-2 is inferior to LJSVD in most cases, indicating that the left shared structure is more powerful since the only difference in experiments between LJSVD and RJSVD-2 is the relative position of the shared components.
- (iii) Although RJSVD-1 does not perform the best, but it still has similar performance toward LJSVD and outperforms RJSVD-2 in most cases (10 out of 12). Considering the only difference between RJSVD-1 and RJSVD-2 is that the HID layers are included for joint decomposition in the former only, we reach to the conclusion that the more layers for joint decomposition, the better the performance, which is consistent with the observation (i).
- (iv) Comparing with LJSVD and RJSVD, Bi-JSVDp, $p = 0.3, 0.5, 0.7$, can achieve not only the highest raw accuracy in most cases but also satisfying final performance. As shown in the Figure 3, the performance of Bi-JSVDp tends to increase with p , but the lines seem to be affected by "noise", which might caused by the difference between the original networks. For example, it is shown that $p = 1$ tends to achieve higher performance in the ResNet-50 or ResNet-34 for CIFAR-10 and CIFAR-100, while the best p in ResNet-18 for CIFAR-10 is 0.7. Thus, there may not be a specific answer for the question left in the last experiment. However, empirically, $p = 1$

can be the first option in deciding p unless the specific evaluating experiment is conducted.

(v) Tucker Decomposition and NC_CTD achieve the highest raw accuracies than other methods in most cases, but fail to achieve the best performance in most cases, indicating the final performance is not strictly linearly correlated with the accuracy before fine-tuning and the structure of the decomposed network may be the key factor. However, for a same single method under different CFs, a smaller CF brings higher raw and final accuracy, thus in this scenario, raw accuracy dose is linearly correlated with final performance.

(vi) There is an particular phenomenon that for ResNet-18 on CIFAR-100, those decomposed networks outperform the original one. The reason for this is that the original CNN is probably over-fitting since all the original networks are trained with the same settings without particular adjustment, and the decomposition alleviates the over-fitting problem as reported in [18].

B. Evaluation on ImageNet

1) *Settings:* To further verify the effectiveness of the proposed methods, We conduct comparison experiments on a large scale data set, ImageNet (ILSVRC12), which contains 1.2 millions images from 1000 classes. For data preprocessing, all the images are normalized with $mean = [0.485, 0.456, 0.406]$ and standard deviation $std = [0.229, 0.224, 0.225]$, and the test images are cropped centrally to 224×224 . For data augmentation, training images are resized to 224×224 using 4 different methods provided by Tensorflow followed by a random horizontal flip.

The ResNet-34 [7] for ImageNet with 21.78 millon of parameters is used for evaluation. For time-saving, the pre-trained weights are downloaded from Pytorch Model Zoo² and transferred to Tensorflow. Fine-tuned with several epochs, the network achieves 71.03% Top-1 accuracy and 90.25% Top-5 accuracy.

LJSVD, RJSVD-1 and Bi-JSVD0.5 are utilized to compress the ResNet-34 following the 'pre-train→decompose→fine-tune' criteria, compared with Tai *et.al* [18] , Tucker [11] and NC_CTD [25]. Following Section IV-A, K for Bi-JSVD is set to be 30, and conv1, conv2_x in ResNet-34 are not decomposed. The proportion of the shared component and the independent one for NC_CTD is set to 1:1. In the fine-tuning period, the SGD is used as optimizer with a momentum of 0.9. The batch size is set to 128, and weights are regularized by L2 with a weight decay of 5e-4. Since it's very time-consuming to fine-tune ResNet-34 for ImageNet, the warmup strategy [7][37] is applied to accelerate the fine-tuning process, with which the learning rate for the first 3 epochs are set to 0.0001, 0.001 and 0.01, respectively. After the warmup phase, the compressed networks are fine-tuned for 25 epoch, with the learning rate starts from 0.1 and divided by 10 in the 6th, 11th, 16th and 21th epochs.

2) *Results and analysis:* . The results of all the methods are shown in the TABLE VI. It is shown that for ImageNet classification, the proposed methods can still outperform the state-of-the-art methods and alleviate performance degradation. The Top-1 accuracy of all the proposed methods are more than 2% higher than NC_CTD [25]when CF=10.98, and Bi-JSVD0.5 achieves 0.52% higher Top-5 accuracy comparing to Tai *et.al* [18] when CF is set to be 5.75, which further demonstrates the compatibility of the proposed algorithms and verify the effectiveness of the jointly decomposed methods for network compression.

CNN & acc. (%)	CF (×)	Method	Raw Top-1 acc. (%)	Raw Top-5 acc. (%)	Top-1 acc. (%)	Top-5 acc. (%)
ResNet-34	10.98	Tai <i>et.al</i> [18]	0.15	0.87	60.17	83.27
		Tucker [11]	0.15	0.79	57.64	81.40
		NC_CTD [25]	0.38	1.60	58.37	82.29
		LJSVD	0.24	1.30	60.55	83.68
		RJSVD-1	0.24	1.11	60.74	83.65
		Bi-JSVD0.5	0.13	0.74	60.83	83.58
ResNet-18	5.75	Tai <i>et.al</i> [18]	0.24	0.97	62.52	84.88
		Tucker [11]	0.84	3.09	58.15	81.86
		NC_CTD [25]	0.39	1.67	61.12	84.26
		LJSVD	0.44	1.67	63.36	85.64
		RJSVD-1	0.32	1.51	63.43	85.74
		Bi-JSVD0.5	0.43	1.98	64.12	86.16

Table VI: Comparison of compressed ResNet-34 for ImageNet following the 'pre-train→decompose→fine-tune' criteria.

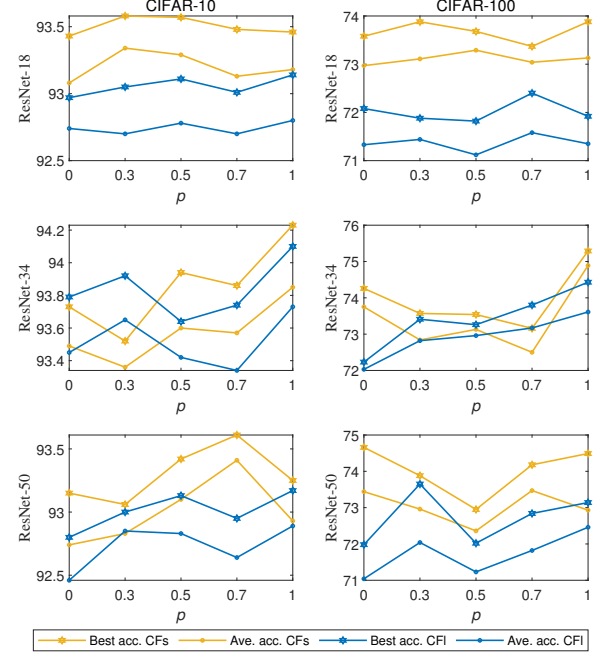


Fig. 4: The performance of Bi-JSVD for CNNs trained from scratch under different p . "Ave. acc.", "Best acc.", "CFs" and "CFI" means Average accuracy, Best accuracy, the smaller CF and the larger one for each CNN shown in the TABLE VII and VIII, respectively.

C. Ablation Study: training from scratch

1) *Settings:* The comparison experiments demonstrates superior performance of the proposed methods, and we consider

²<https://download.pytorch.org/models/resnet34-333f7ec4.pth>.

	CNN & acc. (%)	CF (\times)	Method	Acc. (%) (mean \pm std)	Best acc. (%)
ResNet-18	17.76	Tai <i>et.al</i> [18]	92.66 \pm 0.07	93.10	
		Tucker [11]	90.83 \pm 0.13	91.33	
		NC_CTD [25]	90.77 \pm 0.31	91.56	
		LJSVD	92.80 \pm 0.17	93.14	
		RJSVD-1	92.83\pm0.13	93.14	
		RJSVD-2	92.74 \pm 0.13	92.97	
		Bi-JSVD0.3	92.70 \pm 0.19	93.05	
		Bi-JSVD0.5	92.78 \pm 0.11	93.11	
		Bi-JSVD0.7	92.70 \pm 0.09	93.01	
		Tai <i>et.al</i> [18]	92.73 \pm 0.13	92.94	
ResNet-34	11.99	Tucker [11]	90.94 \pm 0.15	91.33	
		NC_CTD [25]	91.22 \pm 0.13	91.72	
		LJSVD	93.18 \pm 0.11	93.46	
		RJSVD-1	93.35\pm0.01	93.58	
		RJSVD-2	93.08 \pm 0.09	93.43	
		Bi-JSVD0.3	93.34 \pm 0.13	93.58	
		Bi-JSVD0.5	93.29 \pm 0.17	93.57	
		Bi-JSVD0.7	93.13 \pm 0.09	93.48	
		Tai <i>et.al</i> [18]	92.90 \pm 0.03	93.11	
		Tucker [11]	91.83 \pm 0.25	92.31	
ResNet-50	22.07	NC_CTD [25]	91.03 \pm 0.13	91.53	
		LJSVD	93.73\pm0.09	94.10	
		RJSVD-1	93.59 \pm 0.14	94.00	
		RJSVD-2	93.45 \pm 0.15	93.79	
		Bi-JSVD0.3	93.65 \pm 0.13	93.92	
		Bi-JSVD0.5	93.42 \pm 0.09	93.64	
		Bi-JSVD0.7	93.34 \pm 0.15	93.74	
		Tai <i>et.al</i> [18]	93.11 \pm 0.04	93.43	
		Tucker [11]	91.78 \pm 0.15	92.20	
		NC_CTD [25]	91.46 \pm 0.10	91.79	
ResNet-50	6.48	LJSVD	93.85\pm0.19	94.23	
		RJSVD-1	93.62 \pm 0.15	93.62	
		RJSVD-2	93.49 \pm 0.14	93.73	
		Bi-JSVD0.3	93.36 \pm 0.07	93.52	
		Bi-JSVD0.5	93.60 \pm 0.09	93.94	
		Bi-JSVD0.7	93.57 \pm 0.06	93.86	
		Tai <i>et.al</i> [18]	91.99 \pm 0.08	92.42	
		LJSVD	92.89\pm0.11	93.17	
		RJSVD-1	92.77 \pm 0.03	92.97	
		RJSVD-2	92.46 \pm 0.15	92.80	
ResNet-50	5.37	Bi-JSVD0.3	92.85 \pm 0.15	93.00	
		Bi-JSVD0.5	92.83 \pm 0.18	93.13	
		Bi-JSVD0.7	92.64 \pm 0.20	92.95	
		Tai <i>et.al</i> [18]	92.22 \pm 0.19	92.55	
		LJSVD	92.93 \pm 0.15	93.25	
		RJSVD-1	93.00 \pm 0.02	93.37	
		RJSVD-2	92.74 \pm 0.18	93.15	
		Bi-JSVD0.3	92.83 \pm 0.07	93.06	
		Bi-JSVD0.5	93.10 \pm 0.19	93.42	
		Bi-JSVD0.7	93.41\pm0.09	93.61	

Table VII: Comparison of compressed ResNet trained from scratch on CIFAR-10.

that there are two main reasons contributes to their superiority: the joint structures, and prior knowledge inherited from the original networks. To verify this, we further conduct ablation experiments in the way of training decomposed networks from scratch, which also evaluates the ability of the proposed method in compressing CNNs in another manner. This time we retain the structures of the compressed networks as in Section IV-A3 and train them from scratch with random initialization of the parameters. The training settings such as number of epoch, learning rate and batch sizes are consistent with those in Section IV-A3.

	CNN & acc. (%)	CF (\times)	Method	Acc. (%) (mean \pm std)	Best acc. (%)
ResNet-18	16.61	Tai <i>et.al</i> [18]	71.12 \pm 0.35	72.25	
		Tucker [11]	69.67 \pm 0.23	69.88	
		NC_CTD [25]	70.66 \pm 0.27	71.24	
		LJSVD	71.35 \pm 0.19	71.92	
		RJSVD-1	71.59\pm0.39	72.48	
		RJSVD-2	71.33 \pm 0.16	72.08	
		Bi-JSVD0.3	71.44 \pm 0.13	71.88	
		Bi-JSVD0.5	71.12 \pm 0.19	71.82	
		Bi-JSVD0.7	71.58 \pm 0.40	72.40	
		Tai <i>et.al</i> [18]	71.63 \pm 0.25	72.26	
ResNet-34	21.11	Tucker [11]	69.84 \pm 0.29	70.92	
		NC_CTD [25]	70.72 \pm 0.06	71.43	
		LJSVD	73.13 \pm 0.31	73.88	
		RJSVD-1	73.38\pm0.22	73.96	
		RJSVD-2	72.97 \pm 0.51	73.58	
		Bi-JSVD0.3	73.11 \pm 0.23	73.88	
		Bi-JSVD0.5	73.29 \pm 0.09	73.68	
		Bi-JSVD0.7	73.04 \pm 0.11	73.37	
		Tai <i>et.al</i> [18]	72.59 \pm 0.49	73.81	
		Tucker [11]	70.95 \pm 0.51	71.87	
ResNet-50	6.21	NC_CTD [25]	71.52 \pm 0.03	72.14	
		LJSVD	73.61 \pm 0.37	74.43	
		RJSVD-1	73.66\pm0.25	74.14	
		RJSVD-2	72.03 \pm 0.19	72.23	
		Bi-JSVD0.3	72.82 \pm 0.29	73.41	
		Bi-JSVD0.5	72.96 \pm 0.05	73.26	
		Bi-JSVD0.7	73.17 \pm 0.21	73.80	
		Tai <i>et.al</i> [18]	73.60 \pm 0.11	73.85	
		Tucker [11]	70.88 \pm 0.07	71.48	
		NC_CTD [25]	71.38 \pm 0.15	72.25	
ResNet-50	5.19	LJSVD	74.89\pm0.19	75.29	
		RJSVD-1	74.38 \pm 0.31	74.95	
		RJSVD-2	73.75 \pm 0.12	74.26	
		Bi-JSVD0.3	72.84 \pm 0.17	73.57	
		Bi-JSVD0.5	73.13 \pm 0.29	73.54	
		Bi-JSVD0.7	72.50 \pm 0.35	73.16	
		Tai <i>et.al</i> [18]	70.32 \pm 0.27	70.91	
		LJSVD	72.46\pm0.31	73.14	
		RJSVD-1	71.93 \pm 0.41	72.76	
		RJSVD-2	71.40 \pm 0.20	71.98	
ResNet-50	75.67	Bi-JSVD0.3	72.04 \pm 0.83	73.65	
		Bi-JSVD0.5	71.23 \pm 0.26	72.02	
		Bi-JSVD0.7	71.82 \pm 0.43	72.84	
		Tai <i>et.al</i> [18]	71.35 \pm 0.38	72.02	
		LJSVD	72.93 \pm 0.97	74.49	
		RJSVD-1	72.81 \pm 0.45	73.68	
		RJSVD-2	73.44 \pm 0.11	74.66	
		Bi-JSVD0.3	72.96 \pm 0.78	73.88	
		Bi-JSVD0.5	72.36 \pm 0.22	72.95	
		Bi-JSVD0.7	73.47\pm0.36	74.18	

Table VIII: Comparison of compressed ResNet trained from scratch on CIFAR-100.

2) *Results:* The results are shown in the Table VII and VIII, and the Figure 4 shows how p affects the performance of compressed networks.

3) *Analysis:* Not surprisingly, the proposed methods still achieves performance better than the baselines, which demonstrates the power of the propose joint structures on alleviating performance degradation. Conclusions similar to the previous subsection can still be summarized, however, there are some outcomes different from the previous results as follows:

(i) Comparing these results with those in the Table IV and V, the accuracy obtained by each method drops in different degrees in most cases, implying that factorized weights inheriting the prior knowledge from the original

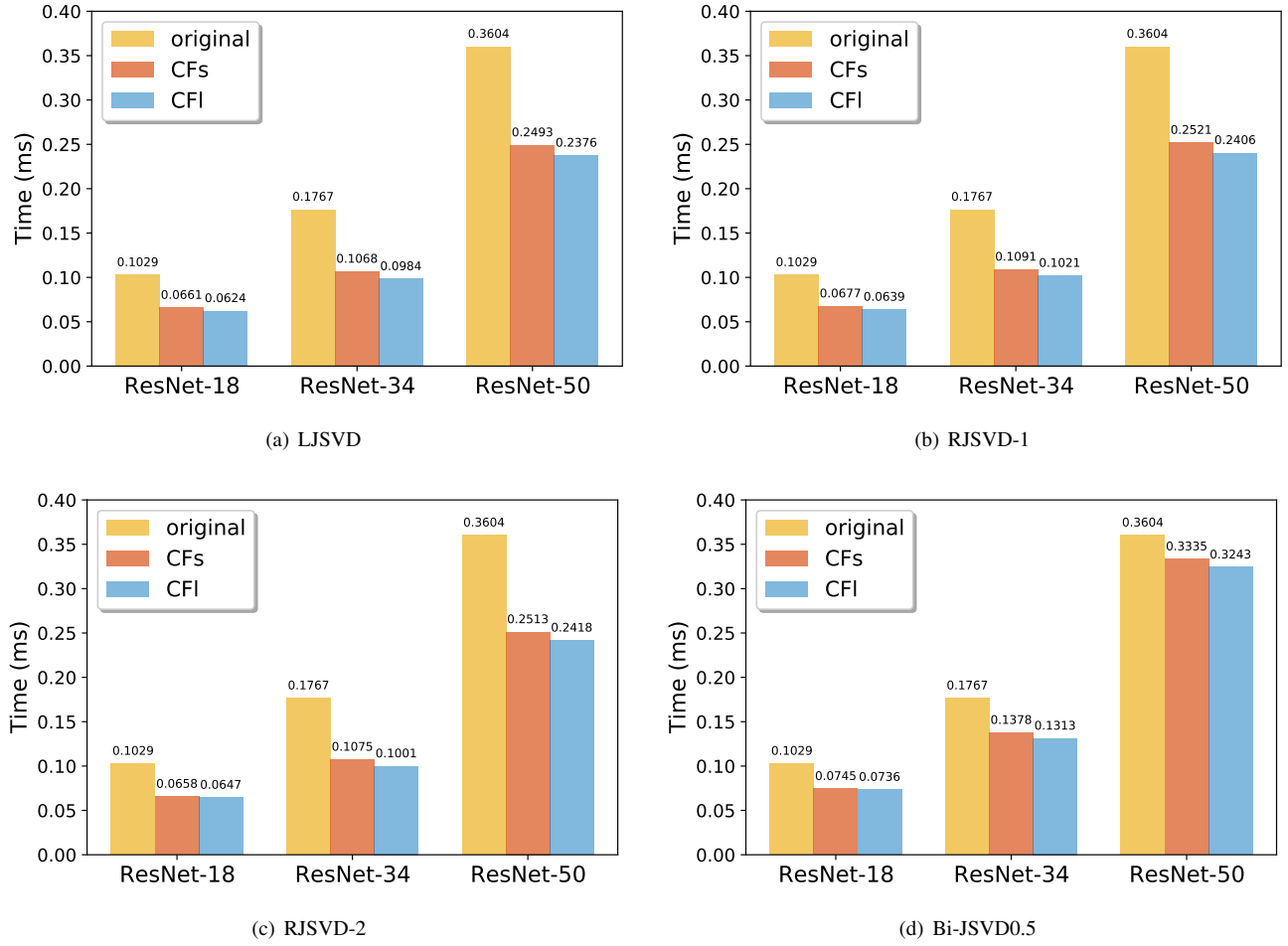


Fig. 5: Realistic acceleration on the forward procedure for CIFAR-10. "CFs" means the smaller CF for each CNN shown in the Table IV while "CFI" means the larger one.

networks give a better initialization to help CNNs settling at a better local minimum. Furthermore, the drops for the proposed methods are much smaller than the baselines in most cases, further verifying the advantages of the proposed methods. For example, LJSVD outperforms Tai *et.al*'s method with 2.14% higher accuracy across ResNet-50 on CIFAR-100 when CR = 6.21, while it is 0.68% in the experiments with the 'pre-train→decompose→fine-tune' criteria. This observation demonstrates that the proposed methods are more initialization-independent, and thus the joint structures is the main factor in improving performance.

(ii) Different from results shown in the Figure 3, the curves in each sub-figure of the Figure 4 are more messy and have no obvious trends, indicating that compressed networks under the 'pre-train→decompose→fine-tune' criteria are trained following specific patterns decided by the original networks, whereas the ones trained from scratch are in random.

D. Realistic Acceleration

1) *Settings*: As mentioned in the Section III, the complexity of a compressed convolutional layer produced by the proposed

methods are less than the original layer, thus the forward inference can be accelerated. But there is a wide gap between the theoretical and realistic acceleration, which is restricted by the IO delay, buffer switch, efficiency of BLAS libraries [38] and some indecomposable layers such as batch normalization and pooling. Therefore, to evaluate the realistic acceleration fairly, we measure the real forward time of the networks compressed by LJSVD, RJSVD-1, RJSVD-2, and Bi-JSVD0.5 in TABLE IV. Each experiment is conducted on a TITAN Xp GPU by setting the batch size to 500, and the measurement is repeated for 5 times to calculate the average time cost for one image.

2) *Results and analysis*: As shown in the Figure 5, all the networks are accelerated even though there is no support from particular libraries. LJSVD, RJSVD-1 as well as RJSVD-2 have similar encouraging acceleration achievement especially on ResNet-18 and ResNet-34, while Bi-JSVD is not as outstanding as them. The reason for this is that there is a double parallel inferences among a compressed layer in Bi-JSVD, as in the Figure 2, which consumes more time. Since the ResNet-50 is built with BottleNeck included 1×1 convolutional layer, the acceleration on ResNet-50 is less obvious as that on ResNet-18 and ResNet-34. Furthermore, it is shown that the degrees of acceleration under the relatively larger and

smaller CFs are similar, although there is a relatively great gap between CFs such as $8.15\times$ in ResNet-34, which means the time consumption caused by the IO delay, buffer switch and efficiency of BLAS libraries and some indecomposable layers as mentioned above accounts for a huge proportion.

V. CONCLUSION AND FUTURE WORK

In this paper, inspired by the fact that there are repeated modules among CNNs, we propose to compress networks jointly to alleviate performance degradation, and three joint matrix decomposition algorithms, RJSVD, LJSVD and Bi-JSVD, which is a generalization of the first two, are introduced. Extensive experiments on CIFAR-10, CIFAR-100 and the larger scale ImageNet show that our methods can achieve better compression result comparing with the state-of-the-art matrix or tensor based methods, and the speed acceleration in the forward inference period is verified as well.

In future work, we plan to extend the joint method to other area such as network structured pruning to push the acceleration on CNNs to a higher stage, and use techniques for AutoML such as Neural Architecture Search [39], Reinforcement Learning [40] and Evolutionary Algorithms [41][42] to estimate the best p for Bi-JSVD as well as target ranks and compress networks adaptively.

REFERENCES

- [1] J. Guan, R. Lai, A. Xiong, Z. Liu, and L. Gu, “Fixed pattern noise reduction for infrared images based on cascade residual attention CNN,” *Neurocomputing*, vol. 377, pp. 301–313, 2020.
- [2] F. Taherkhani, H. Kazemi, and N. M. Nasrabadi, “Matrix completion for graph-based deep semi-supervised learning,” in *AAAI*. AAAI Press, 2019, pp. 5058–5065.
- [3] R. B. Girshick, J. Donahue, T. Darrell, and J. Malik, “Rich feature hierarchies for accurate object detection and semantic segmentation,” in *CVPR*. IEEE Computer Society, 2014, pp. 580–587.
- [4] H. Purwins, B. Li, T. Virtanen, J. Schlüter, S. Chang, and T. N. Sainath, “Deep learning for audio signal processing,” *IEEE J. Sel. Top. Signal Process.*, vol. 13, no. 2, pp. 206–219, 2019.
- [5] X. X. Zhu, S. Montazeri, M. Ali, Y. Hua, Y. Wang, L. Mou, Y. Shi, F. Xu, and R. Bamler, “Deep learning meets SAR,” *CoRR*, vol. abs/2006.10027, 2020.
- [6] K. Simonyan and A. Zisserman, “Very deep convolutional networks for large-scale image recognition,” in *ICLR*, 2015.
- [7] K. He, X. Zhang, S. Ren, and J. Sun, “Deep residual learning for image recognition,” in *CVPR*. IEEE Computer Society, 2016, pp. 770–778.
- [8] S. Zagoruyko and N. Komodakis, “Wide residual networks,” in *BMVC*. BMVA Press, 2016.
- [9] S. Xie, R. B. Girshick, P. Dollár, Z. Tu, and K. He, “Aggregated residual transformations for deep neural networks,” in *CVPR*. IEEE Computer Society, 2017, pp. 5987–5995.
- [10] M. Tan and Q. V. Le, “Efficientnet: Rethinking model scaling for convolutional neural networks,” in *ICML*, ser. Proceedings of Machine Learning Research, vol. 97. PMLR, 2019, pp. 6105–6114.
- [11] Y. Kim, E. Park, S. Yoo, T. Choi, L. Yang, and D. Shin, “Compression of deep convolutional neural networks for fast and low power mobile applications,” in *ICLR*, 2016.
- [12] A. Jain, P. Goel, S. Aggarwal, A. Fell, and S. Anand, “Symmetric k -means for deep neural network compression and hardware acceleration on fpgas,” *IEEE J. Sel. Top. Signal Process.*, vol. 14, no. 4, pp. 737–749, 2020.
- [13] F. N. Iandola, M. W. Moskewicz, K. Ashraf, S. Han, W. J. Dally, and K. Keutzer, “SqueezeNet: Alexnet-level accuracy with 50x fewer parameters and <1mb model size,” *CoRR*, vol. abs/1602.07360, 2016.
- [14] B. Wu, F. N. Iandola, P. H. Jin, and K. Keutzer, “SqueezeDet: Unified, small, low power fully convolutional neural networks for real-time object detection for autonomous driving,” in *CVPR Workshops*. IEEE Computer Society, 2017, pp. 446–454.
- [15] M. Denil, B. Shakibi, L. Dinh, M. Ranzato, and N. de Freitas, “Predicting parameters in deep learning,” in *NIPS*, 2013, pp. 2148–2156.
- [16] E. L. Denton, W. Zaremba, J. Bruna, Y. LeCun, and R. Fergus, “Exploiting linear structure within convolutional networks for efficient evaluation,” in *NIPS*, 2014, pp. 1269–1277.
- [17] M. Jaderberg, A. Vedaldi, and A. Zisserman, “Speeding up convolutional neural networks with low rank expansions,” in *BMVC*. BMVA Press, 2014.
- [18] C. Tai, T. Xiao, X. Wang, and W. E, “Convolutional neural networks with low-rank regularization,” in *ICLR (Poster)*, 2016.
- [19] A. Novikov, D. Podoprikhin, A. Osokin, and D. P. Vetrov, “Tensorizing neural networks,” in *NIPS*, 2015, pp. 442–450.
- [20] V. Lebedev, Y. Ganin, M. Rakuba, I. V. Oseledets, and V. S. Lempitsky, “Speeding-up convolutional neural networks using fine-tuned cp-decomposition,” in *ICLR (Poster)*, 2015.
- [21] T. Garipov, D. Podoprikhin, A. Novikov, and D. P. Vetrov, “Ultimate tensorization: compressing convolutional and FC layers alike,” *CoRR*, vol. abs/1611.03214, 2016.
- [22] W. Wang, Y. Sun, B. Eriksson, W. Wang, and V. Aggarwal, “Wide compression: Tensor ring nets,” in *CVPR*. IEEE Computer Society, 2018, pp. 9329–9338.
- [23] X. Yu, T. Liu, X. Wang, and D. Tao, “On compressing deep models by low rank and sparse decomposition,” in *CVPR*. IEEE Computer Society, 2017, pp. 67–76.
- [24] J. Huang, W. Sun, and L. Huang, “Deep neural networks compression learning based on multiobjective evolutionary algorithms,” *Neurocomputing*, vol. 378, pp. 260–269, 2020.
- [25] W. Sun, S. Chen, L. Huang, H. C. So, and M. Xie, “Deep convolutional neural network compression via coupled tensor decomposition,” *IEEE J. Sel. Top. Signal Process.*, vol. 15, no. 3, pp. 603–616, 2021.
- [26] I. V. Oseledets, “Tensor-train decomposition,” *SIAM J. Sci. Comput.*, vol. 33, no. 5, pp. 2295–2317, 2011.
- [27] Q. V. Le, A. Karpenko, J. Ngiam, and A. Y. Ng, “ICA with reconstruction cost for efficient overcomplete feature learning,” in *NIPS*, 2011, pp. 1017–1025.
- [28] M. Sun, D. Snyder, Y. Gao, V. K. Nagaraja, M. Rodehorst, S. Panchapagesan, N. Strom, S. Matsoukas, and S. Vitaladevuni, “Compressed time delay neural network for small-footprint keyword spotting,” in *INTERSPEECH*. ISCA, 2017, pp. 3607–3611.
- [29] S. Swaminathan, D. Garg, R. Kannan, and F. Andrès, “Sparse low rank factorization for deep neural network compression,” *Neurocomputing*, vol. 398, pp. 185–196, 2020.
- [30] J. Guo, Y. Li, W. Lin, Y. Chen, and J. Li, “Network decoupling: From regular to depthwise separable convolutions,” in *BMVC*. BMVA Press, 2018, p. 248.
- [31] C. Szegedy, W. Liu, Y. Jia, P. Sermanet, S. E. Reed, D. Anguelov, D. Erhan, V. Vanhoucke, and A. Rabinovich, “Going deeper with convolutions,” in *CVPR*. IEEE Computer Society, 2015, pp. 1–9.
- [32] A. G. Howard, M. Zhu, B. Chen, D. Kalenichenko, W. Wang, T. Weyand, M. Andreetto, and H. Adam, “Mobilennets: Efficient convolutional neural networks for mobile vision applications,” *CoRR*, vol. abs/1704.04861, 2017.
- [33] B. Wu, D. Wang, G. Zhao, L. Deng, and G. Li, “Hybrid tensor decomposition in neural network compression,” *Neural Netw.*, vol. 132, pp. 309–320, 2020.
- [34] I. Goodfellow, Y. Bengio, and A. Courville, *Deep Learning*. MIT Press, 2016.
- [35] A. Krizhevsky and G. Hinton, “Learning multiple layers of features from tiny images,” Tech. Rep., 2009.
- [36] J. Zhou, H. Qi, Y. Chen, and H. Wang, “Progressive principle component analysis for compressing deep convolutional neural networks,” *Neurocomputing*, vol. 440, pp. 197–206, 2021.
- [37] P. Goyal, P. Dollár, R. B. Girshick, P. Noordhuis, L. Wesolowski, A. Kyrola, A. Tulloch, Y. Jia, and K. He, “Accurate, large minibatch SGD: training imagenet in 1 hour,” *CoRR*, vol. abs/1706.02677, 2017.
- [38] Y. He, P. Liu, Z. Wang, Z. Hu, and Y. Yang, “Filter pruning via geometric median for deep convolutional neural networks acceleration,” in *CVPR*. Computer Vision Foundation / IEEE, 2019, pp. 4340–4349.
- [39] X. Dong and Y. Yang, “Nas-bench-201: Extending the scope of reproducible neural architecture search,” in *ICLR*. OpenReview.net, 2020.
- [40] V. Mnih, K. Kavukcuoglu, D. Silver, A. A. Rusu, J. Veness, M. G. Bellemare, A. Graves, M. A. Riedmiller, A. Fidjeland, G. Ostrovski, S. Petersen, C. Beattie, A. Sadik, I. Antonoglou, H. King, D. Kumaran, D. Wierstra, S. Legg, and D. Hassabis, “Human-level control through deep reinforcement learning,” *Nat.*, vol. 518, no. 7540, pp. 529–533, 2015.

- [41] K. Deb, S. Agrawal, A. Pratap, and T. Meyarivan, "A fast and elitist multiobjective genetic algorithm: NSGA-II," *IEEE Trans. Evol. Comput.*, vol. 6, no. 2, pp. 182–197, 2002.
- [42] Q. Zhang and H. Li, "Moea/d: A multiobjective evolutionary algorithm based on decomposition," *IEEE Transactions on Evolutionary Computation*, vol. 11, no. 6, pp. 712–731, 2007.